# Numerical and lab experiment study of a novel concentrating PV with uniform flux distribution

Guiqiang Li[1*], Qingdong Xuan[1], Yashun Lu[1], Gang Pei[1*], Yuehong Su[2], Jie Ji[1]

[1] *Department of Thermal Science and Energy Engineering, University of Science and Technology of China, 96 Jinzhai Road, Hefei City 230026, China*

[2] *Institute of Sustainable Energy Technology, University of Nottingham, University Park, Nottingham NG7 2RD, UK*

[*] Corresponding authors. Tel/Fax: +86 551 63607367. E-mail: ligq@mail.ustc.edu.cn; peigang@ustc.edu.cn

**Abstract:** The uniform illumination profile that falls on the PV cell is good for PV output and lifespan, however the flux distribution of the concentrating PV appears to be non-uniform in most cases which is harmful for the overall performance of the concentrating photovoltaic. In order to overcome this disadvantage, a novel asymmetric compound parabolic concentrator concentrating PV with uniform flux distribution is proposed in this paper. A two-dimensional finite element model is built for electrical performance simulation of the concentrating photovoltaic module. The prototype of the concentrating photovoltaic module is manufactured and assembled to conduct the indoor lab experiment under Standard Test Condition to verify the feasibility and reliability of the model. The outdoor experiments are conducted to show the electrical performance of the concentrating photovoltaic module under the real weather condition. Then the model is used to analyze the electrical performance of the PV cell under the flux distribution created by the proposed concentrator. The results show that the electrical performance of the proposed concentrating photovoltaic module is close to that under the uniform flux distribution with the same total radiation level, which confirms that the proposed concentrator is beneficial for the PV output under concentrating illumination due to uniform flux distribution.

**Keywords:** concentrating photovoltaic (CPV); flux distribution; two-dimensional finite element model; electrical performance

## 1 Introduction

Solar concentrating system can attain a larger solar irradiation than that without solar concentrator. For PV application, solar concentrating system can get a higher flux intensity which can save lots of PV cells and reduce the cost significantly in theory. There are many CPV (concentrating photovoltaic) systems were designed and studied by researchers. Du et al. designed a mirror lens CPV with the active water cooling [1]. Renzi et al. analyzed the performance of two 3.5kWp CPV systems under real operating conditions [2]. Li et al. simulated and tested a low concentrating solar concentrators integrated with building for CPV [3, 4]. Mallick et al. designed an asymmetric concentrator in the specular reflection or total internal reflection forms for building integrated CPV application [5-7].

However, many solar concentrators can only provide non-uniform flux distribution, which usually have significant impact on the PV output. What’s more, the presence of non-uniformity increases the temperature across some portions of the cells and causes hotspots which will finally intensify material aging and thus tend to deteriorate the cell performance. As the concentration ratio increases, it will become more difficult to maintain uniformity of the flux on the solar cells. In Coventry's study, an experiment comparison was conducted on a single solar cell in both uniform and non-uniform flux distribution. The results showed that there is a reduction in open circuit voltage of 6.5 mV and an obvious deviation of *I-V* curves is observed under the uniform and non-uniform illumination conditions, and the author pointed out an efficiency drop from 20.6% with uniform illumination to 19.4% with non-uniform illumination [8, 9]. Katz et al. [10] produced a localized illumination for a 100 $mm^2$ triple-junction GaInP2 /GaAs/Ge cell with the uniform front metallization with the total power varies from 0.1 W to 8 W. The experiment results indicated that the open voltage, fill factor and PV cell efficiency all got a decline affected by the local illumination compared with the uniform illumination. Manor et al. [11] conducted the experiment for the large photoactive area organic cell with poly (3-hexylthiophene) (P3HT)/PCBM BHJ under the uniform and localized illumination and the results showed that a decline of the open voltage was observed between the localized and uniform illumination.

On the contrary, there are many precedents of improving the performance of the concentrators by flatten the flux illumination profile that falls on the receiver of the concentrator where the PV cell is attached. Li et al. [12] concluded that the lens-walled CPC (compound parabolic concentrator) whose flux distribution is more uniform than the normal mirror CPC shows higher fill factor values and the experiment certified their conclusions. Wang et al. [13] proposed that for the tube receiver with parabolic trough collector system, decreasing the heat flux gradient and peak magnitude on the receiver can reduce the thermal stress and avert receiver failure. Hatwaambo et al. [14] demonstrated that the fill factor of the low concentrating CPCs can be improved by a semi-diffuse aluminum sheet reflector with rolling grooves oriented parallel to the plane of the solar cell module due to more uniform flux distribution across the solar cell.

Franklin and Coventry [9] indicated that the parabolic trough concentrator has the Gaussian flux profile on the cell. Li et al presented that the lens concentrator has also a non-uniform distribution [15]. Some methods can also be considered to improve the flux distribution, such as the use of active or passive cooling mechanisms [16-18], use of high-grade silicon solar cells, and/or the use of semi-diffuse reflectors [14] on the already existing concentrator geometries have been tried. Huang et al indicated that when the receiver plane is placed somewhat upwards or downwards from the focus, the Fresnel solar concentrator can improve the uniformity of flux distribution [19]. Secondary optical elements can also be used to weaken negative effects of the non-uniformity [20, 21]. Perez-Enciso et al. [22] proposed a method to achieve a uniform flux distribution with a multi-faceted point focus concentrator, however for most of solar concentrators, the uniformity of flux distribution is still an inevitable problem.

Compound parabolic concentrators are the typical solar concentrator with Gaussian flux profile which is a promising concept for it can works with a fixed installation. The high solar irradiation can make solar cells produce larger amounts of currents, but the non-uniform illumination lowers the efficiency due to the losses caused by the increase in series resistance. Mammo et al. [23] revealed that efficiency deviation is mainly due to the non-uniform illumination distribution.

In order to overcome this disadvantage, and the need of achieving homogenous flux distribution on photovoltaic, thermal or other kind of receivers in solar concentrating devices is a common issue. Thus, this paper displayed a novel concentrating PV with uniform flux distribution. It is found through the ray tracing simulation that the flux distribution of the proposed novel concentrating PV is very uniform with the variance value of 0.327 which is much more uniform than that of the normal symmetric mirror CPC whose variance value is 4.764 with the same geometric concentration ratio. Through the simulation and experiment, the modeled *I-V* curves for the PV cell under the uniform flux distribution and that under the flux distribution created by the proposed concentrator show a good agreement, which indicates that the electrical performance of the concentrating PV module is close to that under the uniform flux distribution with the same total radiation level. The study proves the benefits of the proposed concentrator for the output improvement of the solar cells under concentrating illumination. As for the cost of the proposed CPV module, It was demonstrated by Mallick et al. that for the low-concentration dielectric compound concentrator PV technology, a reduction of the overall system cost of up to 53% could be expected in volume production instead of the small number of systems currently manufactured though the cost of the dielectric concentrator may outweigh the PV material cost savings, especially when the price of PVs has fallen significantly [6]. And the material quality of the concentrator proposed in the paper is only 1/4–1/5 of that of the dielectric concentrator, so it can further reduce the cost as well as the weight.

## 2 The CPV module

### 2.1 The geometry

The geometry of the proposed concentrator is designed in the asymmetric structure as shown in Fig. 1, which is composed of the asymmetric compound parabolic curves in the form of the lens structure and mirrors. An air gap is set between the lens and mirrors, thus the sun rays can be collected either by the total internal reflection or by the specular reflection, which will increase the optical performance of the concentrator. For the further structure optimization, the concentrator is designed by rotating the original concentrator around the up end point of the absorber M by a certain degree $\lambda$ which means that the incidence angle for the original concentrator $\theta$ will be $\theta'$ for the optimization concentrator: $\theta'=\theta-\lambda$. The optimization structure of the concentrator integration with PV is detailed studied in the paper. The angle between the normal of the absorber and the incident ray is defined as the incidence angle for the proposed concentrator. The geometric concentration ratio ($C$) is 2.4x, which is defined as: Aperture width/Absorber width.

2.2 The layout form of the CPV module

The structure shown in Fig. 2 is the layout form of the concentrating PV module where the PV cell is attached to the absorber of the concentrator. Some key position parameters of the CPV module can be concluded as: the rotation angle of the concentrator is 5° and the concentrator is titled at 10° (the angle between the normal of *M'N'* and the incident ray). In the following sections, the optical and electrical performance of the CPV module at this layout form is detailed presented.

## 3 Simulation analysis and discussions

3.1 The optical performance of the CPV module

The software Lighttools® is used to perform the ray tracing simulation for the proposed concentrator thus to find out the optical efficiencies and flux distribution on the absorber of the concentrator. Lighttools® is a fast and accurate ray-tracing photometric analysis program which provides the optical system modeling and performance evaluation for non-imaging optical design.

During the simulation process, the material of the concentrator is set as PMMA and the specular reflectivity is set to be 85%. The number of total incident rays is

10000 and the intensity of the solar radiation is 1000 $Wm^{-2}$. All the incidence rays are assumed to be parallel and the schematic diagram of the ray tracing simulation is shown in Fig. 3.

The optical efficiencies of the proposed concentrator at varies incidence angles are depicted in Fig. 4. From the results, it can be seen clearly that the optical efficiency is very high within the acceptance range of 0-60°, the average value of which is 86.6%.

Through the ray tracing simulation, the flux distribution on the absorber of the proposed concentrator and the normal symmetric mirror CPC with the same geometric concentration ratio of 2.4x can be obtained. The flux distributions for two types of CPCs are shown in Fig. 5. The variance value of the averaged local concentration ratios is used to evaluate the uniformity of the flux distribution. From the results, the average value of the local concentration ratios of the proposed concentrator is 2.2, which means that the concentrator can increase the solar radiation on the PV by a factor of 2.2x but the variance value of the results is only 0.327 which indicates that the non-uniformity of the illumination profile is very small. As for the normal symmetric mirror CPC, the average value of the local concentration ratios is 2.07 which is lower than that of the proposed concentrator, and the variance value of the results is 4.764 which is much larger than that of the proposed concentrator. Above all, it’s clearly that the optical efficiency of the proposed concentrator is larger than that of the symmetric mirror CPC, and the flux distribution of the proposed concentrator is also much more uniform than that of the symmetric mirror CPC, which means that the proposed concentrator is definitely a better choice for the better concentrating PV output.

### 3.2 PV simulation by a two-dimensional finite element model

#### 3.2.1 PV cell

The PV cell that is used for the CPV model is shown in Fig.6, which consists of 6 unbroken and 2 segmental emitter regions, 7 fingers in PV cell length direction and 1finger in PV cell width direction and 1 bus-bar. The whole PV cell is modeled by considering the flux distribution that produced by the proposed concentrator at the specific incidence angle under the actual working condition. A comprehensive and accurate comparison with the lab experiment results is conducted to validate the model. The detailed parameters under STC (standard test condition) of the PV cell are shown in table 1.

#### 3.2.2 Illumination profiles

From the flux distribution analysis (given in the averaged local concentration ratio) of the proposed concentrator mentioned above, it's obvious that the flux distribution of the proposed concentrator is very uniform, thus in the following section, the electrical performance of the proposed CPV module is detailed analyzed to verify the benefits for the PV output under the concentrating illumination.

The flux distribution of the uniform distribution and the flux distribution of the CPV module profiles ($G(x)$) in the cell bus-bar direction is shown in Figure. 7. The flux distribution of CPV module is derived by the ray tracing simulation, and the mean illumination on the PV cell for both cases is 2.2 suns. It should be noted that the non-uniform illumination in the bus-bar direction is considered only, which is determined by the joint way between the proposed concentrator and the PV cell, and the various factors that lead to the non-uniform illumination in the finger direction will not be considered in this article.

### 3.2.3 Mathematical modelling

Since the DC current flow in a conductive medium is dealt with, the Partial Differential Equation (PDE) to be solved in the domain is the continuity equation,

$$-\nabla \cdot \left(\sigma \nabla V - J^{e}\right) = Q_{j} \tag{1}$$

Where $V$ is the electric potential, V; $J^{e}$ is the current density, Am$^{-2}$; $Q_j$ is the current source term, Am$^{-3}$; and $\sigma$ is the sheet conductivity of the material which is defined as,

$$\sigma = 1/(R_{sh} \cdot t_{e}) \tag{2}$$

Where $R_{sh}$ is the sheet resistance, $\Omega$; $t_e$ is the depth of the emitter, m.

The current source $Q_j$ is interpreted to be generated by the diode. Thus, the one diode model is used because according to Van. et al. [24], more accurate values can be found for all parameters for such a model. The $Q_j$ can be expressed by eq. (3) with considering the photo-generated current, recombination, and shunts [25],

$$Q_{j} = C_{1}G + C_{2}T^{3}\exp\left(\frac{-E_{g}}{k_{b}T}\right)\left[\exp\left(\frac{q_{e}V_{j}}{nk_{b}T}\right) - 1\right] + C_{3}V_{j} \tag{3}$$

And in the dark bus-bar and finger regions is expressed by

$$Q_{j} = C_{2}T^{3}\exp\left(\frac{-E_{g}}{k_{b}T}\right)\left[\exp\left(\frac{q_{e}V_{j}}{nk_{b}T}\right) - 1\right] + C_{3}V_{j} \tag{4}$$

Where $G$ is the illumination with profile described; $T$ is the cell temperature; $E_g$ is the band gap energy; $k_b$ is the Boltzmann constant; $q_e$ is the electron charge; $V_j$ is the junction electric potential; $n$ is the diode ideality factor; and $C_1$, $C_2$ and $C_3$ are coefficients specific to a given cell (see [26] and reference therein).

3.2.4 Boundary conditions

There are three types of boundary conditions will be considered in this simulation study as shown below [26, 27],

Interface condition: $-n_b \cdot \left( J_1 - J_2 \right) = 0$ (5)

Electric insulation: $n_b \cdot J = 0$ (6)

Bus-bar electric potential: $V = V_{cell}$ (7)

Where $n_b$ is the unit normal to the boundary; $J_1$ and $J_2$ are the current density vectors at the boundary of the adjacent media; and $J$ is the current density vector at the external boundary.

The interface condition is used to ensure the continuity of the current at interfaces between the different media at all internal boundaries; Electric insulation is considered within the areas of the longitudinal outside edges of the bus-bar and external boundaries of the emitter section; the external load is considered to be connected with the ends of the bus-bar which therefore should have the same electric potential as the cell operating voltage $V_{cell}$, an input parameter [26, 27].

## 4. Experimental validation and analysis

### 4.1 Model validation

In order to validate the model, the prototype was manufactured and fabricated as shown in Fig. 8. The indoor lab experiment is conducted under a solar simulator (Oriel Sol3A Model 90943A) from Newport Corporation which generates a ray intensity of 1000 W/m$^2$ (uniform illumination is less than 2% in an active area of 100 x 100 mm$^2$), and the lab experiment setup is shown in Fig. 9. The ambient temperature is 25 ℃.

With the experiment results of the proposed CPV module, the input parameters for the numerical simulation can be identified, which is detailed summarized in Table 2. It should be noted that during the simulation, the temperature on the whole PV cell is set to be 298K in corresponding with the experiment test.

The experimental and modeled *I-V* curves for the proposed CPV module are shown in Fig 10. From the results, it can be seen clearly that the experiment and simulation results show a good agreement, and the deviation of the short circuit current ($I_{sc}$) and open circuit voltage ($V_{oc}$) is very small. However, the maximum power ($P_{\max}$) of the experiment is smaller than the simulation result, which causes the deviation of the *I-V* curves. The values of the maximum power for the experiment and simulation results are 278.982 mW and 299.462 mW respectively, which delivers a relative deviation of 6.68%. The deviation of that can be explained as follows: in the numerical simulation, the ideal CPV model is considered, however actually, there are all kinds of errors that may lead to the deviation. These errors can be concluded as: on the one hand, for the optical concentrators, the performance degradation is a common phenomenon due to all kinds of errors, such as: manufacturing errors which caused imperfect surfaces as compared with the designed concentrator (structure malformation), and imperfect polishing on the concentrator's surfaces; coating errs; the deviation of the concentrator and the PV cell (When soldering the concentrator on the PV cell base, assembly errors existed); on the other hand, test errors due to the test instruments accuracy and artificial errors are inevitable. The influence of the manufacture errors may be significant especially when the concentrator is designed in the form of the total internal reflection because the total internal reflection depends largely on the quality of the concentrator's interface. There were precedents of these errors influencing the optical performance of the concentrators which have been analyzed by many researchers. Mammo et al. conducted both electrical and optical performance analysis for the reflective 3D crossed compound parabolic concentrating photovoltaic system, and the experimental characterization of the optical efficiency was found to show a deviation of 19.4% from the 3D ray tracing simulation results [23]. Abu-Bakar, et al. [28] evaluated the performance of the asymmetrical compound parabolic concentrator and an average deviation of 11% was observed between the experiment results and the simulation results. In conclusion, the simulation results are basically corresponding with the lab experiment results, thus the feasibility and reliability of the model are verified.

## 4.2 The comparison of the PV performance under the uniform flux distribution and the flux distribution created by the proposed concentrator

In this section, the PV cell model described above is used to investigate the electrical performance comparison of the PV cell under the uniform flux distribution and the flux distribution created by the proposed concentrator to analyze the performance of the CPV module and its benefits for the PV output under the concentrating illumination condition due to the relatively uniform flux distribution on the PV cell.

### 4.2.1 The comparison of *I-V* curves

The flux distribution profiles are presented in Fig. 7, and the average flux intensity per surface area is same for both of them [29]. The modeled *I-V* curves for the uniform flux distribution and the flux distribution created by the proposed concentrator are plotted in Fig. 11. A good agreement is observed between the two modeled *I-V* curves and there is a very small difference but can’t be displayed in the figure, which indicates that the electrical performance of the PV cell under the illumination profile created by the proposed concentrator is close to that under the uniform illumination profile with the same total radiation level. Thus, it can be concluded that the proposed concentrator can increase the solar radiation that falls on the PV cell by a ratio of 2.2X, non-uniformity of which can be totally ignored thus to increase the electrical performance of the concentrating PV cell that can be used in various areas.

4.2.2 The comparison of the surface voltage distribution

The voltage distribution on the PV cell surface under the open-circuit condition for the uniform flux distribution and the flux distribution created by the proposed concentrator are shown in Fig. 12. It can be seen from the results that for the uniform flux distribution, the voltage is almost same on the whole PV surface with a largest difference value of 0.0005 V, which may be caused by the layout of the fingers and bus-bar. For CPV module, the difference value between the largest voltage and the lowest voltage on the PV cell surface is 0.009V, which deliveries a relative difference ratio of 1.42%. The voltage tendency through the cell is due to “distributed diode effects”, which can be concluded as: the lateral resistances in the cell leads to a voltage drop across the cell surface, causing different positions on the cell surface to operate at different voltages and therefore produce different current densities [9].

Thus, although the change tendency of the voltage distribution throughout the PV surface under the flux distribution created by the proposed concentrator is a little more obvious than that under the uniform flux distribution, the difference value is very small that it further prove the conclusion drawn from Fig. 11.

4.2.3 The comparison of the current density distribution

The three-dimensional plots of the current density on the PV cell under the short-circuit condition for: (a) uniform flux distribution; (b) flux distribution created by the proposed concentrator are depicted in Fig. 13. The distribution of the current density is proportional to the distribution of the solar intensity, which means that the higher illumination regions have higher current density values. Due to the high conductivity of the finger and the bus-bar and so with neighbouring emitter regions generating almost the same current, the generated current will be absorbed and passed to the fingers and bus-bar directly. Furthermore, the emitter resistance causes a junction voltage which increases with the distance from the finger. As a result, the regions closer to the finger contribute a higher net current to the cell's output, which is called as the "current-crowding". Thus, the positions closer to the finger and bus-bar have a higher current density. Moreover, there can also be a component of minority carrier diffusion laterally through the bulk, which further reduces the current density from positions distance from the fingers and bus-bar as detailed discussed by Aberle et al. [30] but is not fully accounted for in this model. So in conclusion, the nearer to the finger, the higher the current density will be, and the peak value always appears in the closer regions of the fingers and bus-bar for both illumination conditions.

As for the larger peak values in the edge regions of the PV cell (the width of the area is 2 mm) can be concluded as: there is no fingers in this region, the nearest finger is the finger in the bus-bar direction which is vertical to the other 7 fingers. Therefore, the generated current will be absorbed by this vertical finger only while in other emitter regions with the same width, the generated current will be absorbed equally by the fingers on the either side, so the peak values are larger in this edge region than those in other emitter regions. The current density in the fingers and bus-bar is not plotted, because of the great difference of the conductivity between the emitter region and the bus-bar and finger, which will make the current intensity profile in the emitter regions difficult to be visualized if the current intensity in the finger and bus-bar is included in Fig. 13.

From the results shown in Fig. 13, the current density distribution on the PV cell under the uniform flux distribution is more uniform than that under the flux distribution created by the absorber. However, it’s clearly that the peak values in the emitter regions are almost at the same level but only at some regions show a decreases that result in the three-dimensional plot of the current density is not as smooth as that under the uniform flux distribution. The decrease mainly occurs at the left and middle side of the PV cell, this can be explained by: the average solar intensity in these regions is lower than the average value through the whole cell (Fig. 5, Fig. 7), thus the current density which is proportional to the solar intensity will be a little lower.

4.2.4 Overall comparison for the experiment and simulation results

As shown in table 3, there are the five parameters such as $V_{oc}$, $I_{sc}$, $P_m$, $FF$, PV cell efficiency for the CPV module under the experimental test and the numerical simulation. It should be noted that for the concentrating PV cell, the efficiency of it is gotten by: the maximum power ($P_m$)/the total solar radiation that enters the aperture of the concentrator (rather than the actual energy that the PV cell captures). From the results, it can be seen that the difference values of five parameters between the uniform flux distribution and the flux distribution created by the absorber is very small, which further verify that the flux distribution of the CPV module is close to the uniform flux distribution that it is beneficial for the concentrating PV output.

Compared with the non-concentrating PV cell, it can be seen that the proposed concentrator can increase the maximum power ($P_m$) by a factor of 1.93x for the simulation results and this value is 1.80x for the experiment results. The decrease of the experiment results as compared with the simulation results is mainly due to the optical loss which is mainly caused by the manufacture errors.

### 4.3 Outdoor experiment tests

In order to find out the electrical performance of the CPV module under the real weather condition and thus further validate the math model established in the paper, we conduct the outdoor experiments with the portable solar module analyzer from RS PRO®, and the tests are on 17th Dec. 2017 at 12:22 (Test 1) and 15:14 (Test 2) respectively. Detailed outdoor test conditions are shown in table 4 and simulation parameters under outdoor test conditions are presented in table 2. Experimental and modeled *I-V* curves for CPV module: (a) under Test 1 condition; (b) under Test 2 condition are shown in Fig. 14. From the results, it can be seen clearly that the experiment and simulation results show a good agreement, and the deviation of the short circuit current ($I_{sc}$) and open circuit voltage ($V_{oc}$) is very small. The same as the indoor lab experiment, the maximum power ($P_{\max}$) of the outdoor experiment is smaller than the simulation result, which causes the deviation of the *I-V* curves. The deviations of the maximum power can be illustrated as: for the outdoor Test 1: the simulation and experiment maximum power are 249.0 mW and 240.3 mW and the relative deviation is 2.40%; for the outdoor Test 2: the simulation and experiment maximum power are 208.1 mW and 198.8 mW and the relative deviation is 4.50%. Thus, through the outdoor experiments validation, the feasibility and reliability of the model are further verified.

## 5 Conclusions

A novel CPC-type CPV module is proposed and detailed analyzed in this paper. A two-dimensional finite element model is used to perform the numerical simulation for the PV to confirm the benefits of the CPV module proposed in the paper due to the relative uniform flux distribution. The whole PV cell is modeled by considering the flux distribution that produced by the proposed concentrator to make a more comprehensive and accurate comparison with the lab experiment results to validate the model that is used for the numerical simulation. Furthermore, the numerical simulation results are presented to compare the PV performance difference under the flux distribution created by the concentrator and the uniform flux distribution with the same total radiation level. The key conclusions are as follows:

(1) The flux distribution of the proposed concentrator is very uniform with the variance value of 0.327 which is much more uniform than the flux distribution of the normal symmetric mirror CPC whose variance value is 4.764 with the same geometric concentration ratio and the optical efficiency of it is as high as 91.8%;

(2) A good agreement is observed between the experimental and modeled *I-V* curves, and the deviation is mainly caused by the manufacture errors of the concentrator, which verify the feasibility and reliability of the model that is used for the numerical simulation;

(3) The modeled *I-V* curves for PV under the uniform flux distribution and the flux distribution created by the concentrator show a good agreement, which indicates that the electrical performance of the CPV module proposed in the

paper is close to that under the uniform flux distribution with the same total radiation level.

(4) From the comparison of the voltage distribution and the current density distribution on the PV cell for the uniform flux distribution and the flux distribution created by the absorber, it further proves the non-uniformity of the proposed concentrator is very small, which is almost close to the uniform flux distribution.

(5) Simulation five parameters of the PV cell under the uniform illumination profile and illumination profile created by the concentrator show little difference, which both increase the maximum power of the PV cell by a ratio of 1.93x as compared with the non-concentrating cell.

Therefore, the concentrating PV module proposed in this paper can work in the uniform flux distribution which is beneficial for the concentrating PV output and shows a promising concept in the low-concentrating PV technology.

**Acknowledgment**

The study was sponsored by the National Science Foundation of China (Grant Nos. 51408578, 51476159, 51611130195), Anhui Provincial Natural Science Foundation (1508085QE96). The authors would like to express special thanks to the Fundamental Research Funds for the Central Universities. The authors would also like to thank School of Mechanical Engineering, Beijing Institute of Technology, and State Key Laboratory of Fire Science, University of Science and Technology of China, for their assistances in the software simulation.

**References:**

**[1]** B. Du, E. Hu, M. Kolhe. Performance analysis of water cooled concentrated photovoltaic (CPV) system. Renewable and Sustainable Energy Reviews, 16 (2012) 6732-6736.

**[2]** M. Renzi, L. Egidi, G. Comodi, Performance analysis of two 3.5 kWp CPV systems under real operating conditions, Applied Energy, 160 (2015) 687-696.

**[3]** G. Li, G. Pei, J. Ji, M. Yang, Y. Su, N. Xu. Numerical and experimental study on a PV/T system with static miniature solar concentrator. Solar Energy, 120 (2015) 565-574.

**[4]** G. Li, G. Pei, J. Ji, Y. Su. Outdoor overall performance of a novel air-gap-lens-walled compound parabolic concentrator (ALCPC) incorporated with photovoltaic/thermal system. Applied Energy, 144 (2015) 214-223.

**[5]** T.K. Mallick, P.C. Eames, T.J. Hyde, B. Norton. The design and experimental characterisation of an asymmetric compound parabolic photovoltaic concentrator for building facade integration in the UK. Solar Energy, 77 (2004) 319-327.

**[6]** T.K. Mallick, P. EAMES. Design and fabrication of low concentrating second generation PRIDE concentrator. Solar Energy Materials and Solar Cells, 91 (2007) 597-608.

**[7]** T.K. Mallick, P.C. Eames, B. Norton. Non-concentrating and asymmetric compound parabolic concentrating building facade integrated photovoltaics: An experimental comparison. Solar Energy, 80 (2006) 834-849.

**[8]** J.S. Coventry. Performance of a concentrating photovoltaic/thermal solar collector. Solar Energy, 78 (2005) 211-222.

**[9]** Franklin E, Coventry J. Effects of highly non-uniform illumination distribution on electrical performance of solar cells. In: 40th annual conference for the Australian New Zealand solar energy society; 2004.

**[10]** E.A. Katz, J.M. Gordon, W. Tassew, D. Feuermann. Photovoltaic characterization of concentrator solar cells by localized irradiation. Journal of Applied Physics, 100(2006)44514.

**[11]** A. Manor, E.A. Katz, R. Andriessen, Y. Galagan. Study of organic photovoltaics by localized concentrated sunlight: Towards optimization of charge collection in large-area solar cells. Applied Physics Letters, 99 (2011) 173305.

**[12]** L. Guiqiang, P. Gang, S. Yuehong, J. Jie, S.B. Riffat. Experiment and simulation study on the flux distribution of lens-walled compound parabolic concentrator compared with mirror compound parabolic concentrator. Energy, 58 (2013) 398-403.

**[13]** W. Fuqiang, T. Jianyu, M. Lanxin, W. Chengchao. Effects of glass cover on heat flux distribution for tube receiver with parabolic trough collector system. Energy Conversion and Management, 90 (2015) 47-52.

**[14]** S. Hatwaambo, H. Hakansson, A. Roos, B. Karlsson. Mitigating the non-uniform illumination in low concentrating CPCs using structured reflectors. Solar Energy Materials and Solar Cells, 93 (2009) 2020-2024.

**[15]** L. Guiqiang, P. Gang, S. Yuehong, W. Yunyun, J. Jie. Design and investigation of a novel lens-walled compound parabolic concentrator with air gap. Applied Energy, 125 (2014) 21-27.

**[16]** Araki K, Uozumi H, Yamaguchi M. A simple passive cooling structure and its heat analysis for 500 X concentrator PV module//Conference Record IEEE photovoltaic specialists conference. IEEE, 2002, 29(1): 1568-1571.

**[17]** Verlinden P, Sinton R A, Swanson R M, et al. Single-wafer integrated 140 W silicon concentrator module//Photovoltaic Specialists Conference, 1991, Conference Record of the Twenty Second IEEE. IEEE, 1991: 739-743.

**[18]** K. Yang, C. Zuo. A novel multi-layer manifold microchannel cooling system for concentrating photovoltaic cells. Energy Conversion and Management, 89 (2015) 214-221.

**[19]** H. Huang, Y. Su, Y. Gao, S. Riffat. Design analysis of a Fresnel lens concentrating PV cell. International Journal of Low-Carbon Technologies, 6 (2011) 165-170.

**[20]** M. Burhan, K.J.E. Chua, K.C. Ng. Simulation and development of a multi-leg homogeniser concentrating assembly for concentrated photovoltaic (CPV) system with electrical rating analysis. Energy Conversion and Management, 116 (2016) 58-71.

**[21]** Q. Huang, L. Xu. Ball lens as secondary optical element for CPV system. Solar Energy, 148 (2017) 57-62.

**[22]** R. Perez-Enciso, A. Gallo, D. Riveros-Rosas, E. Fuentealba-Vidal, C. Perez-Rábago. A simple method to achieve a uniform flux distribution in a multi-faceted point focus concentrator. Renewable Energy, 93 (2016) 115-124.

**[23]** E.D. Mammo, N. Sellami, T.K. Mallick. Performance analysis of a reflective 3D crossed compound parabolic concentrating photovoltaic system for building façade integration. Progress in Photovoltaics: Research and Applications, 21 (2012) 1095-1103.

**[24]** A.S.H. van der Heide, A. Schönecker, J.H. Bultman, W.C. Sinke. Explanation of high solar cell diode factors by nonuniform contact resistance. Progress in Photovoltaics: Research and Applications, 13 (2005) 3-16.

**[25]** Luque, A., Hegedus, S., 2003. Handbook of Photovoltaic Science and Engineering. Wiley.

**[26]** A. Mellor, J.L. Domenech-Garret, D. Chemisana, J.I. Rosell. A two-dimensional finite element model of front surface current flow in cells under non-uniform, concentrated illumination, Solar Energy, 83 (2009) 1459-1465.

**[27]** J. Domenech-Garret. Cell behaviour under different non-uniform temperature and radiation combined profiles using a two dimensional finite element model. Solar Energy, 85 (2011) 256-264.

**[28]** Siti Hawa Abu-Baka, Firdaus Muhammad-Sukki, Daria Freier, et al. Performance analysis of a novel rotationally asymmetrical compound parabolic concentrator, 2015. Applied Energy, 154, 221–231.

**[29]** Zhou H., Su Y., Pei G., Wang Y. A new approach to model concentrating PV cells under non-uniform illumination. Energy Res. J. 2015, in press.

**[30]** Aberle, A. G., Wenham, S. R. and Green, M. A. (1993). A New Method for the accurate measurement of the lumped series resistance of solar cells. IEEE PS Conference Proceedings 1993.

**Figure captions**

**Fig.1.** The geometry of the proposed concentrator and its optimization structure.

**Fig.2.** Layout form of CPV module.

**Fig.3.** Schematic diagram of the ray tracing simulation for the CPV module.

**Fig.4.** Optical efficiencies at various incidence angles.

**Fig.5.** Averaged local concentration ratios for the proposed concentrator (Distance is counted from L in Fig. 1) and the normal mirror CPC. (Results are derived from the same incidence angle for both kinds of concentrators).

**Fig.6.** PV cell in the experiment.

**Fig.7.** Illumination profiles for: (a) uniform flux distribution; (b) flux distribution of the CPV module in the bus-bar direction.

**Fig.8.** The prototype of the proposed CPV module.

**Fig.9.** The experiment setup.

**Fig. 10.** Experimental and modeled I-V curves for CPV module under STC.

**Fig.11.** Modeled I-V curves for the PV cell under the uniform flux distribution and the flux distribution created by the concentrator.

**Fig.12.** PV cell surface voltage distribution under the open-circuit condition for: (a) uniform flux distribution; (b) flux distribution created by the proposed concentrator. The color data represents the voltage.

**Fig.13.** Three-dimensional plot of the current density on the PV cell under the short-circuit condition for: (a) uniform flux distribution; (b) flux distribution created by the absorber. Both height and color data represent current density. Current density in the fingers and bus-bar is not plotted.

**Fig.14.** Experimental and modeled I-V curves for CPV module: (a) under Test 1 condition; (b) under Test 2 condition.

**Table captions**

**Table 1** Parameters of the PV cell under STC.

**Table 2** Input parameters used in all simulations.

**Table 3** Experiment and simulation results.

**Table 4** Outdoor test conditions.

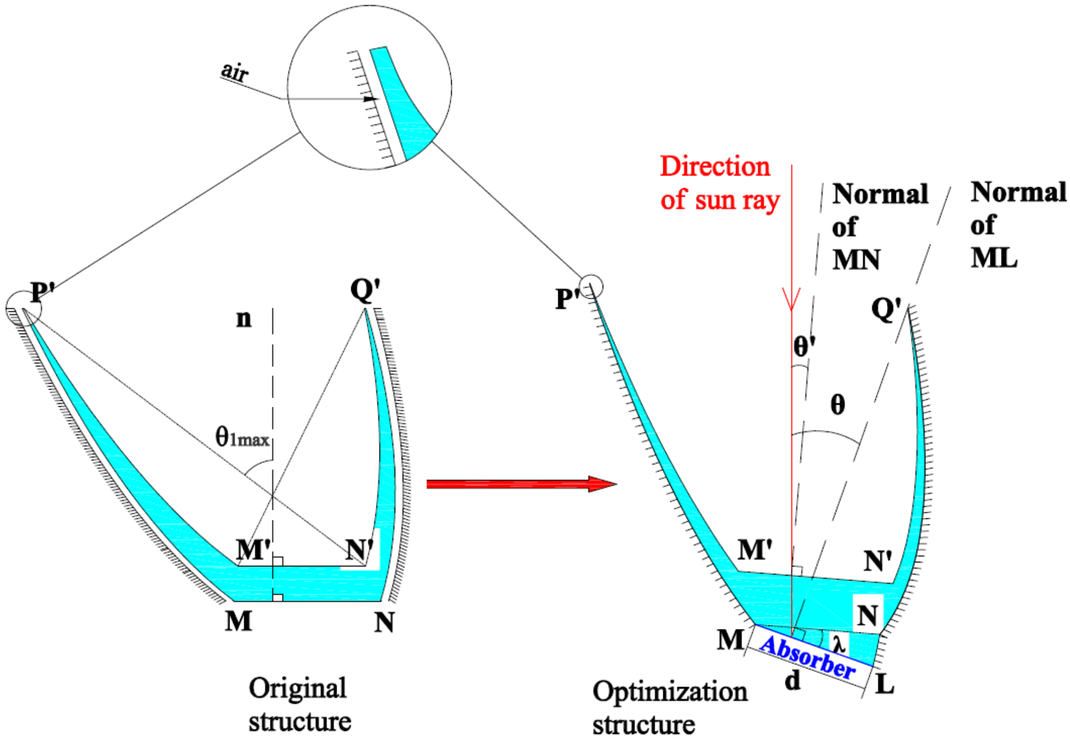


**Fig.1.** The geometry of the proposed concentrator and its optimization structure.

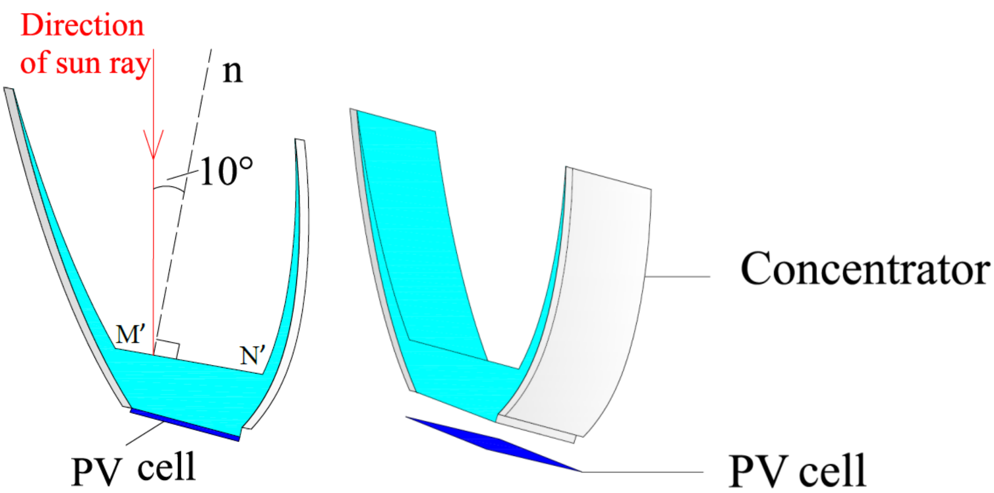


**Fig. 2.** Layout form of CPV module.

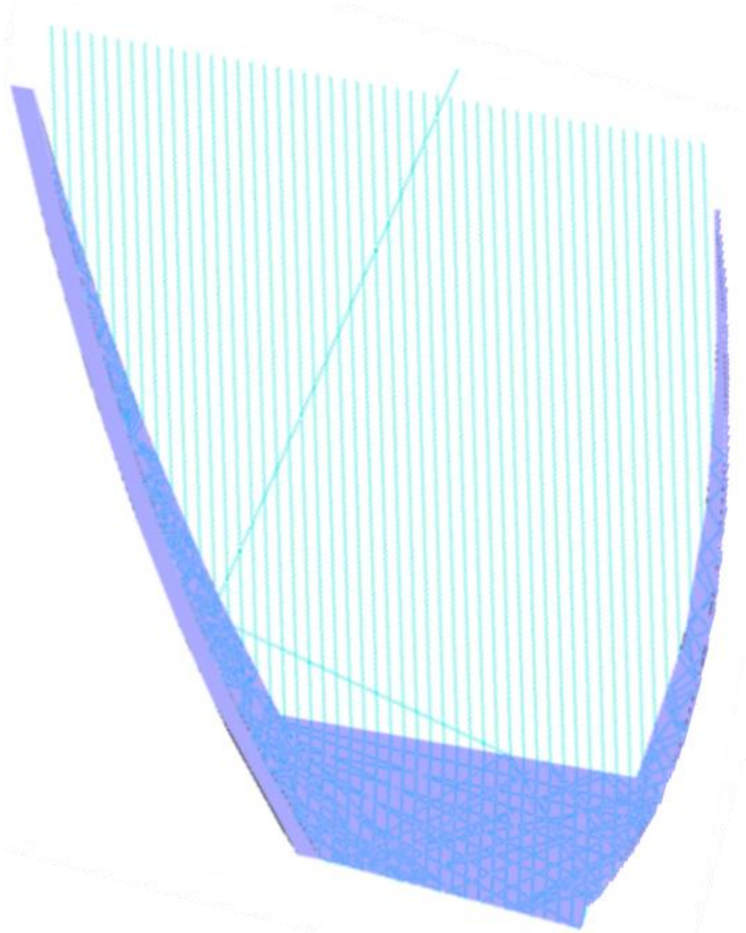

**Fig. 3.** Schematic diagram of the ray tracing simulation for the CPV module.

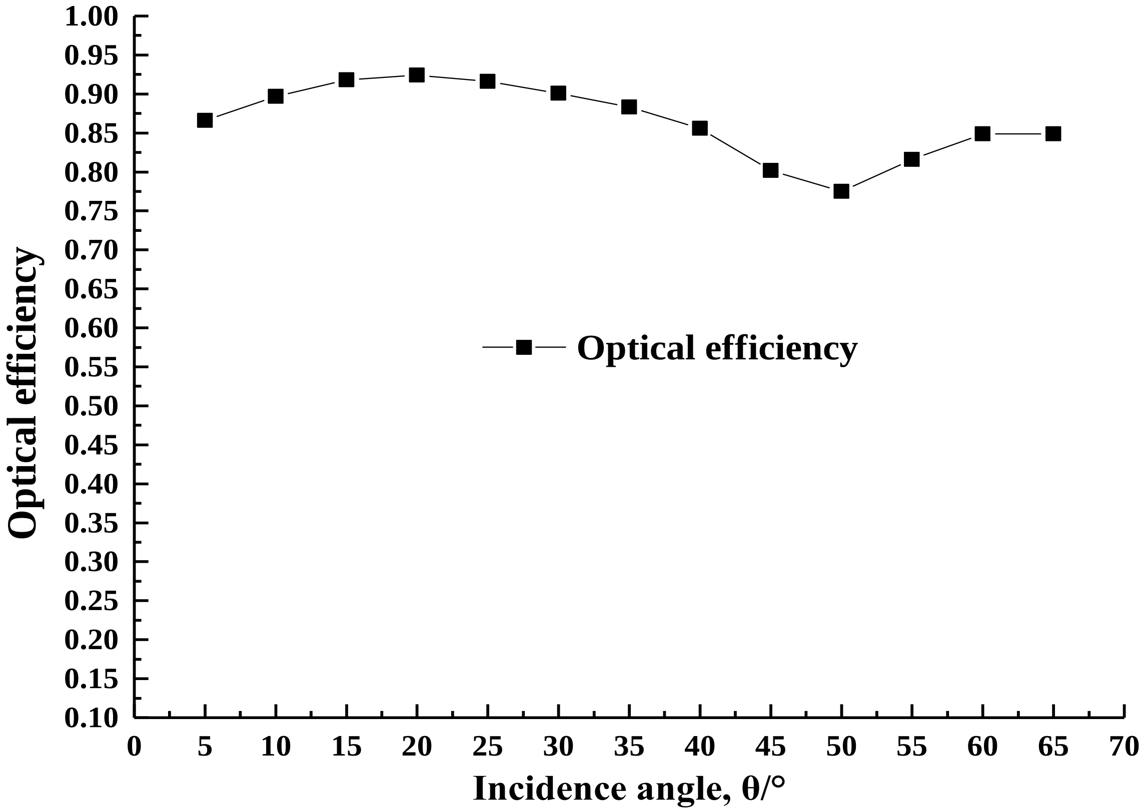


**Fig. 4.** Optical efficiencies at various incidence angles.

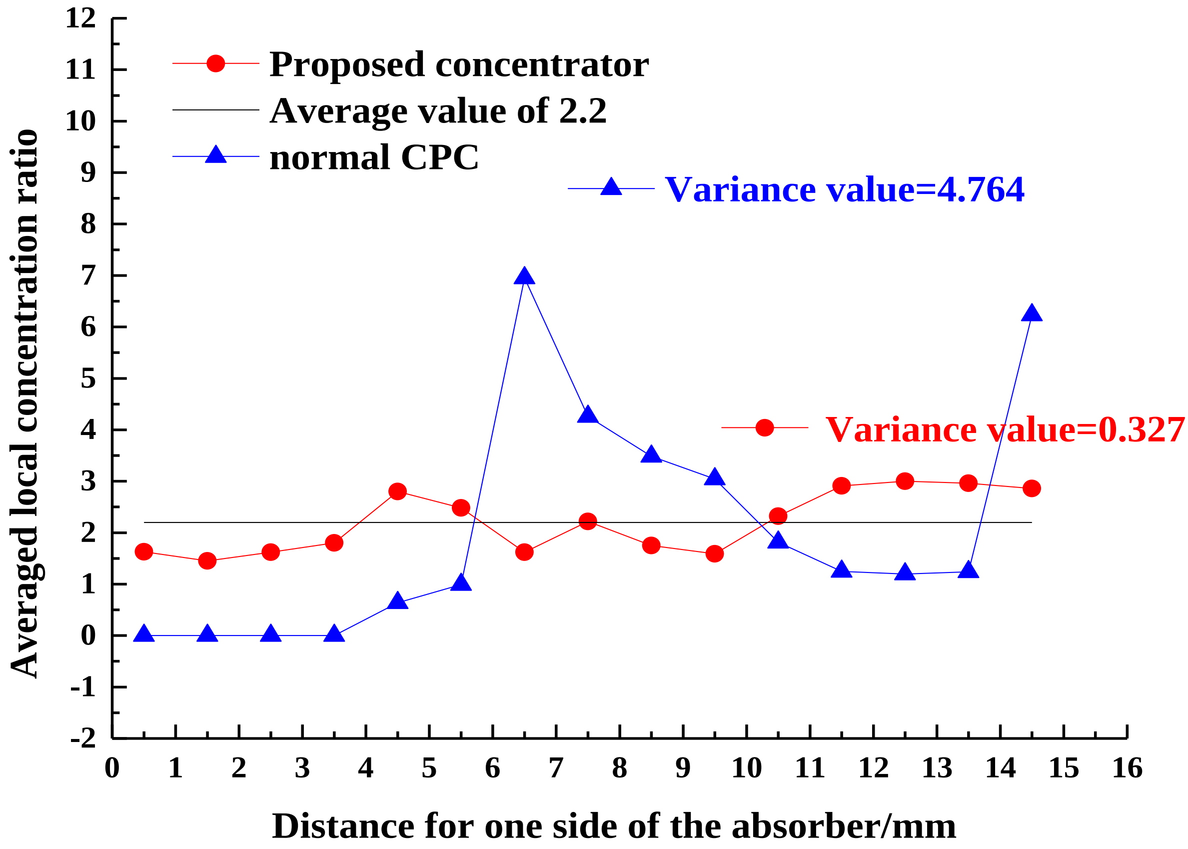


**Fig. 5.** Averaged local concentration ratios for the proposed concentrator (Distance is counted from L in Fig. 1) and the normal mirror CPC. (Results are derived from the same incidence angle for both kinds of concentrators).

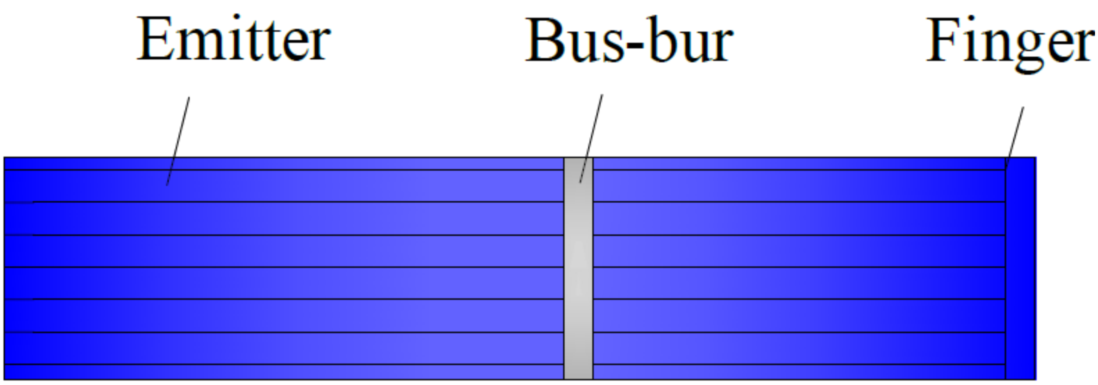


**Fig. 6.** PV cell in the experiment

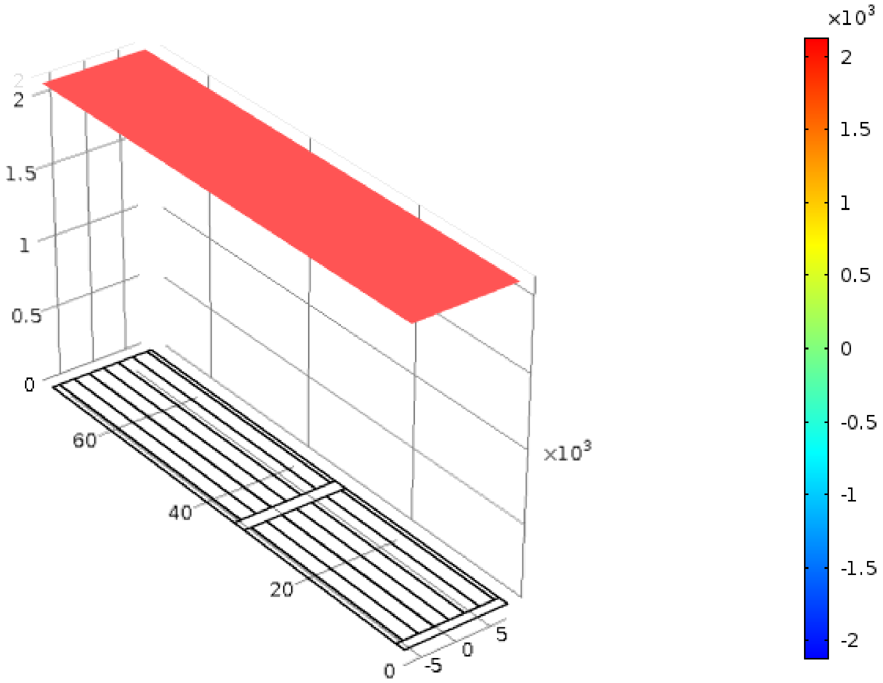


(a)

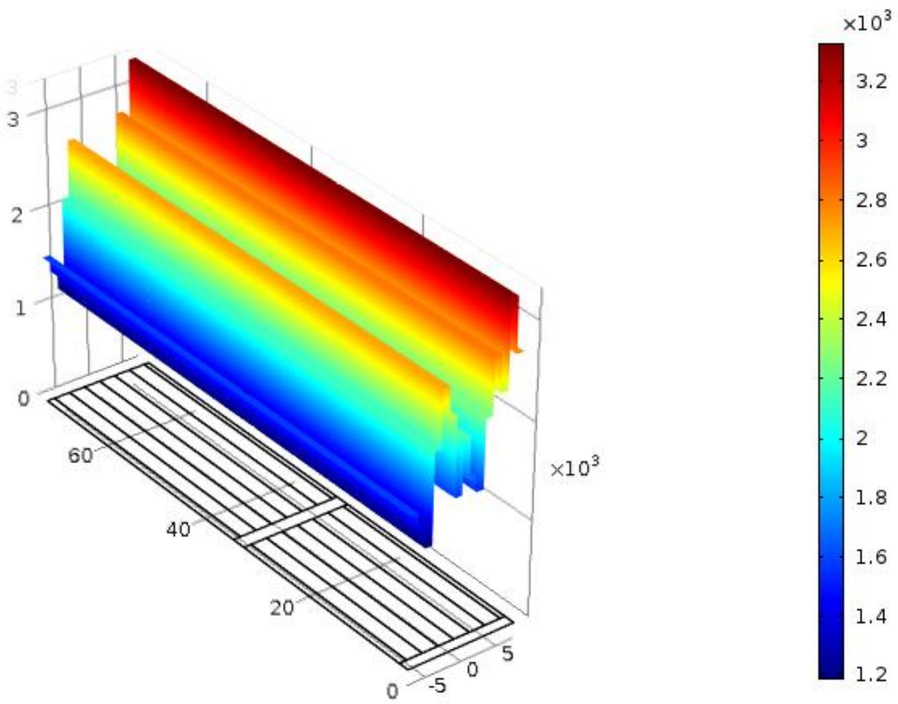


(b)

**Fig. 7.** Illumination profiles for: (a) uniform flux distribution; (b) flux distribution of the CPV module in the bus-bar direction.

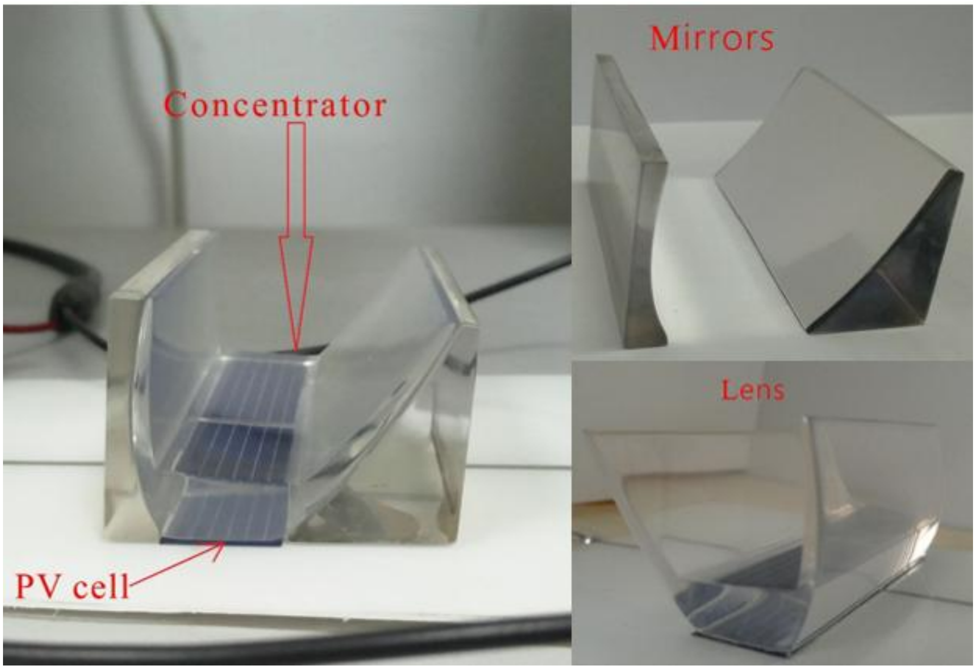


**Fig. 8.** The prototype of proposed CPV module.


**Fig. 9.** The experiment setup.

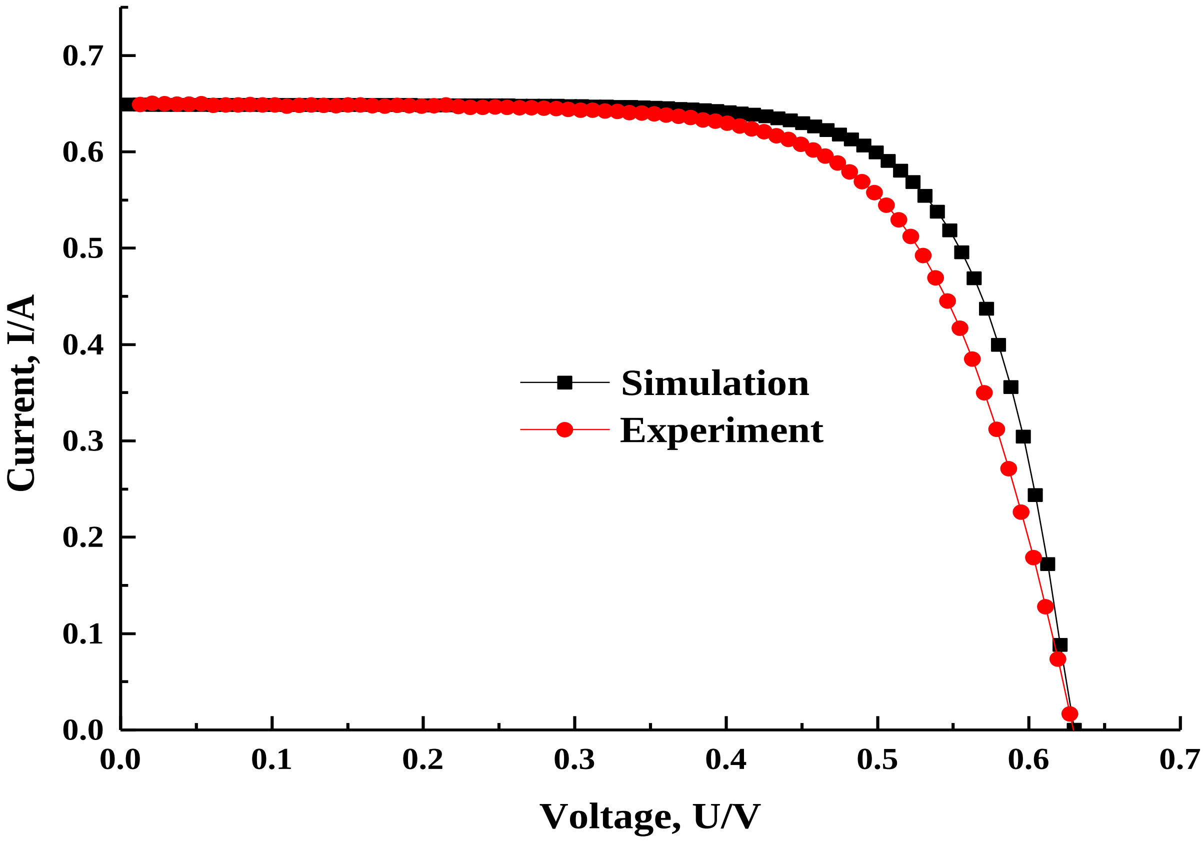


**Fig. 10.** Experimental and modeled I-V curves for CPV module under STC

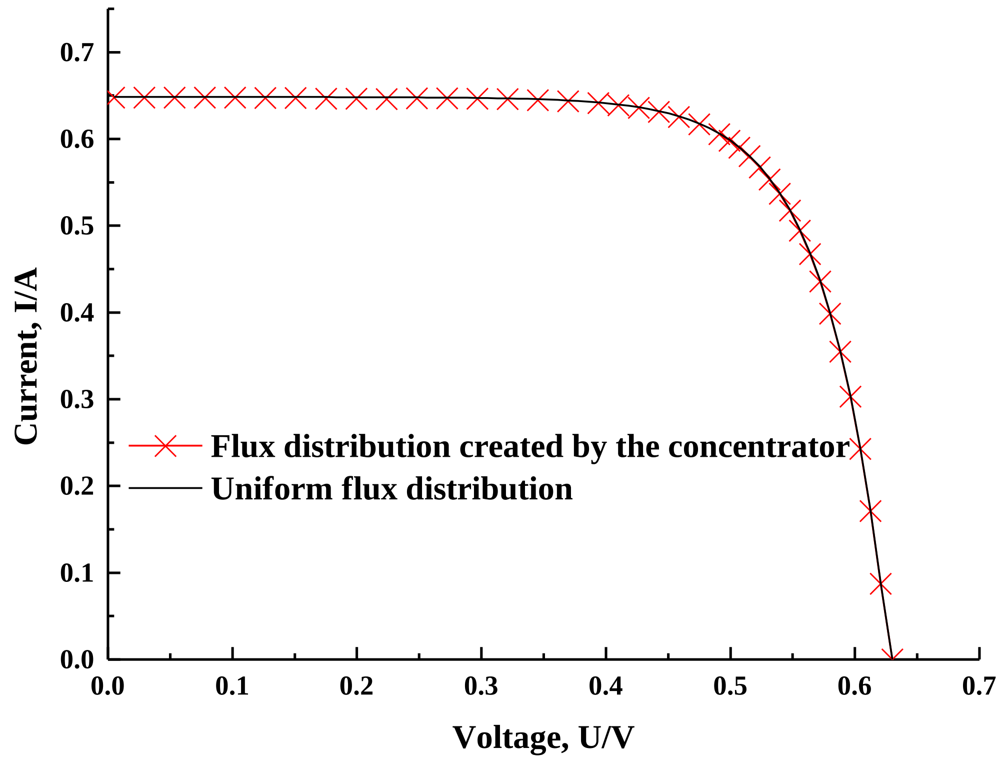


**Fig. 11.** Modeled I-V curves for the PV cell under the uniform flux distribution and the flux distribution created by the concentrator.

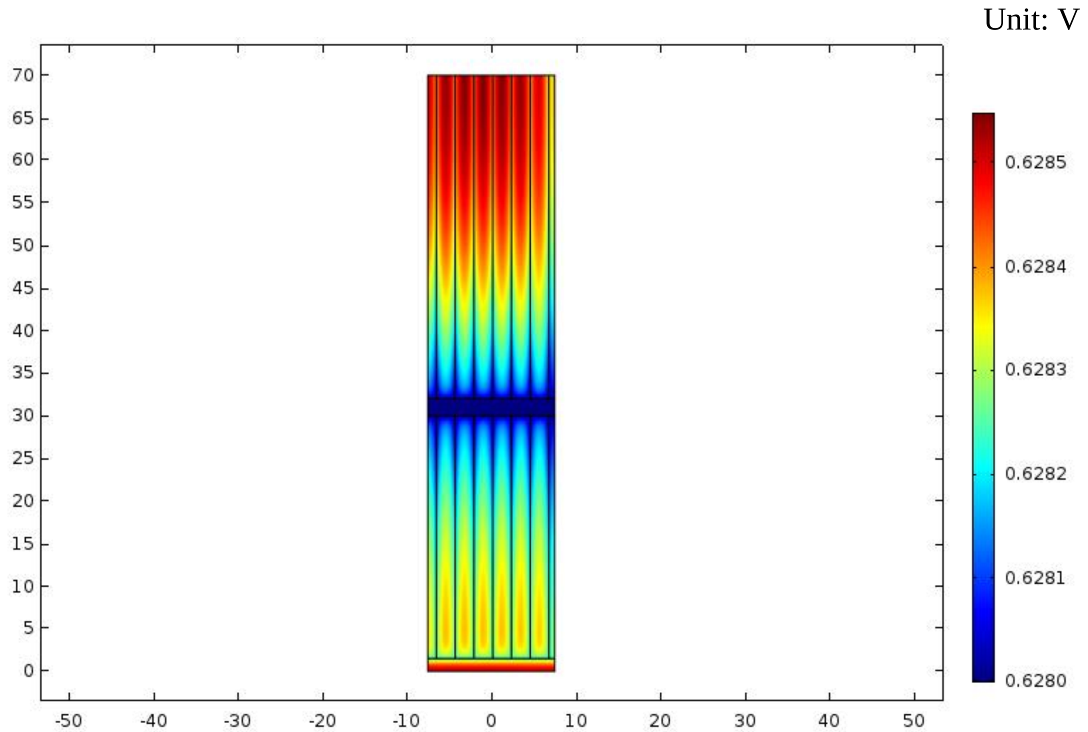


(a)

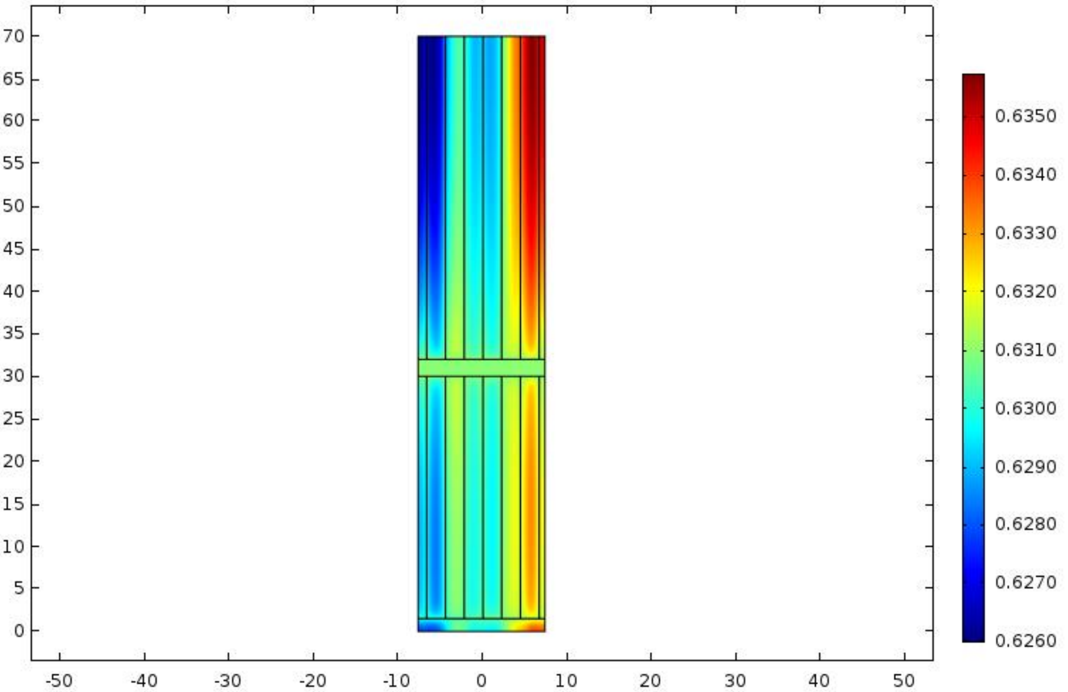


(b)

**Fig. 12.** PV cell surface voltage distribution under the open-circuit condition for: (a) uniform flux distribution; (b) flux distribution created by the proposed concentrator. The color data represents the voltage.

Unit: A

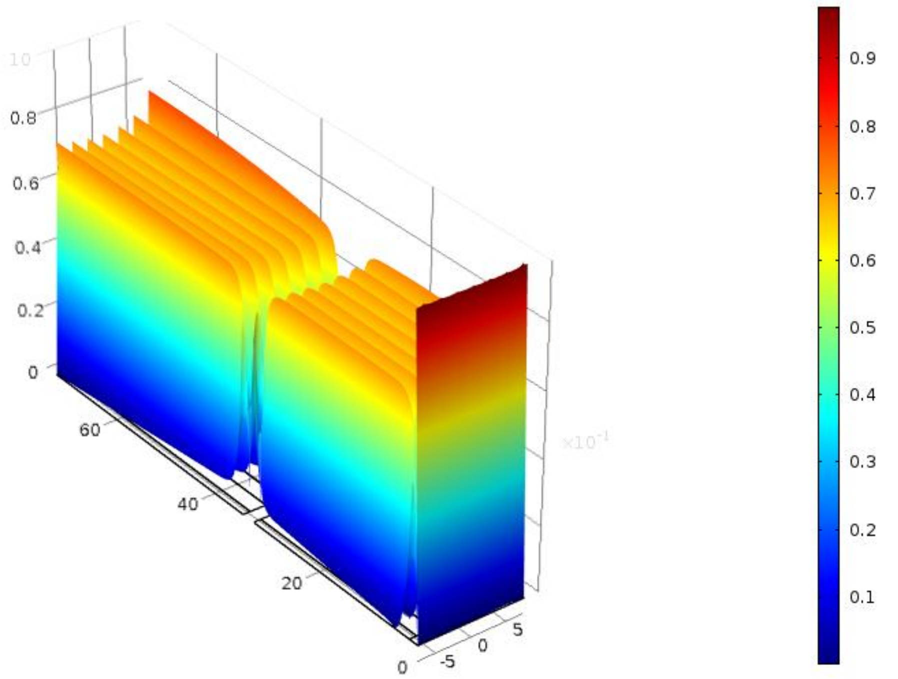


(a)

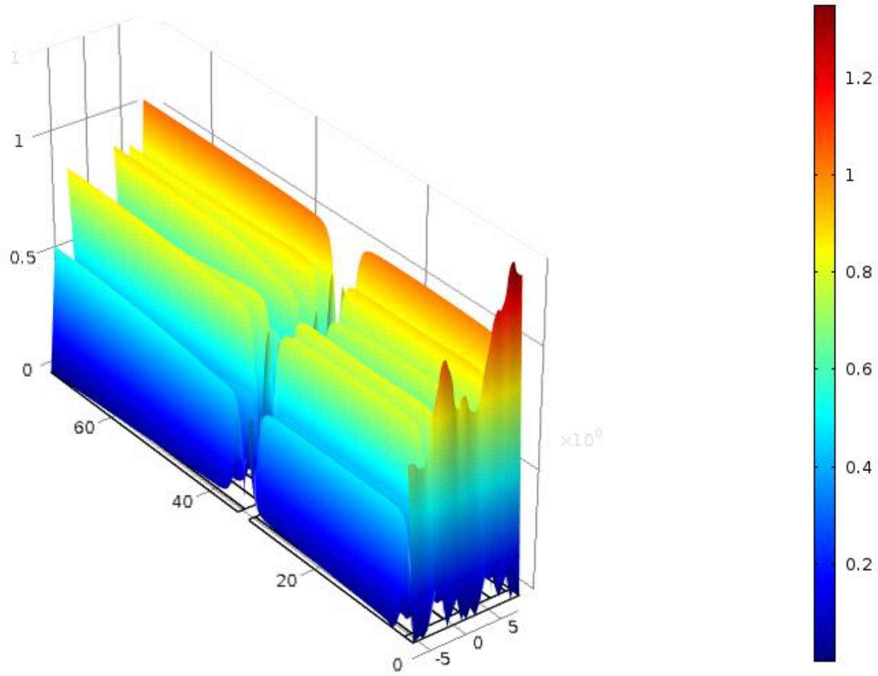


(b)

**Fig.13.** Three-dimensional plot of the current density on the PV cell under the short-circuit condition for: (a) uniform flux distribution; (b) flux distribution created by the absorber. Both height and color data represent current density. Current density in the fingers and bus-bar is not plotted.

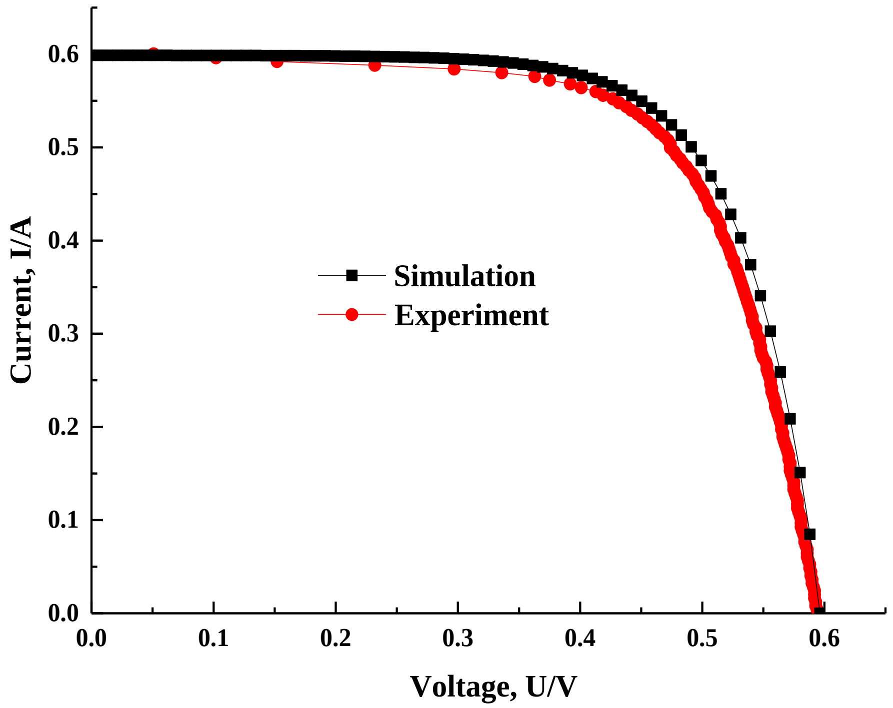


(a)

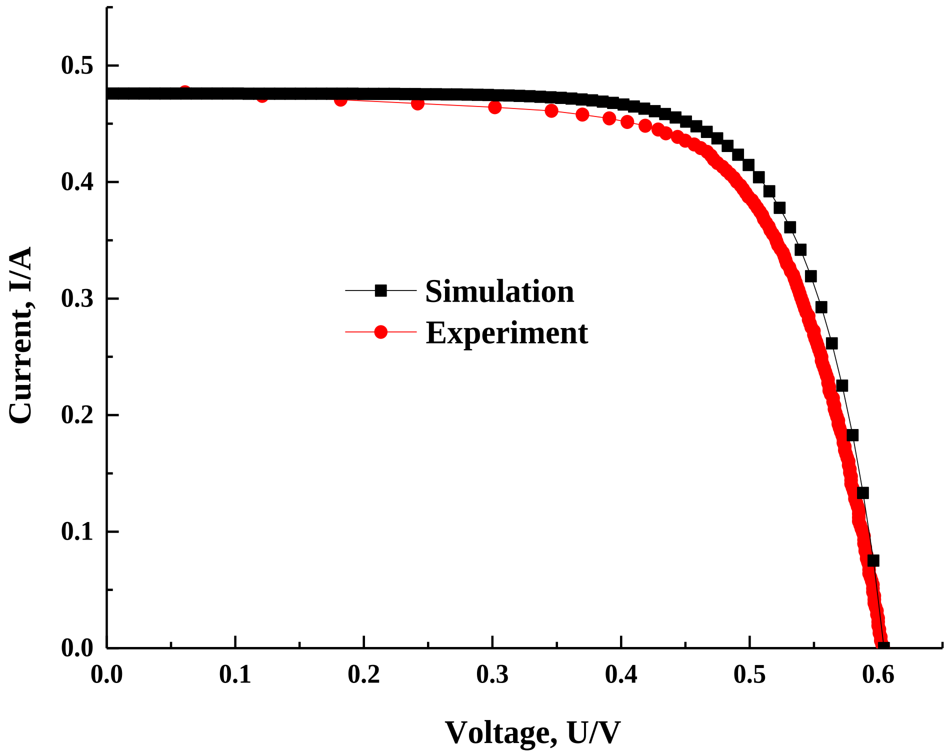


(b)

**Fig.14.** Experimental and modeled I-V curves for CPV module: (a) under Test 1 condition; (b) under Test 2 condition.

**Table 1** Parameters of the PV cell under STC.

| Parameters | Experiment under STC |
|---|---|
| $V_{oc}$ (V) | 0.590 |
| $I_{sc}$ (A) | 0.387 |
| $P_m$ (mW) | 155.619 |
| *FF* (%) | 68.112 |
| *Efficiency* (%) | 15.34 |

**Table 2** Input parameters used in all simulations.

| | | | |
|---|---|---|---|
| *Cell geometry and resistivities* | | | |
| Cell length (finger direction) (cm) | 7 | | |
| Cell width (bus-bar direction) (cm) | 1.5 | | |
| Bus-bar width (mm) | 2 | | |
| Finger width (μm) | 20 | | |
| Finger resistance per unit length ($\Omega$ $cm^{-1}$) | 0.3 | | |
| Emitter sheet resistance ($\Omega$/□) | 100 | | |
| | | *Test conditions* | |
| *Operation conditions* | Indoor | Test 1 | Test 2 |
| Temperature (K) | 298.0 | 280.5 | 280.3 |
| Mean illumination Intensity ($Wm^{-2}$) | 2200.00 | 1571.46 | 1305.48 |
| *Diode equation parameters* | | | |
| $C_1$ ($AW^{-1}$) | 0.3020188 | 0.453753 | 0.37338 |
| $C_2$ ($Am^{-2}K^{-3}$) | -8.14E+08 | -1.58E+11 | -2.82E+10 |
| $C_3$ ($Am^{-2}V^{-1}$) | -1.736953 | -0.146937 | -0.146937 |
| Ideality factor n | 1.938 | 2.4274 | 2.1405 |
| $E_g$ (eV) | 1.124 | 1.124 | 1.124 |

**Table 3** Experiment and simulation results.

| Parameters | Experiment | CPV module | Uniform |
|---|---|---|---|
| $V_{oc}$ (V) | 0.629 | 0.631 | 0.628 |
| $I_{sc}$ (A) | 0.648 | 0.649 | 0.649 |
| $P_m$ (mW) | 278.982 | 299.462 | 299.440 |
| *FF* (%) | 68.421 | 73.136 | 73.508 |
| *Efficiency* (%) | 11.071 | 11.883 | 11.882 |

**Table 4** Outdoor test conditions.

| | Location | Time/Date | Wind speed/ $ms^{-1}$ | Solar radiation/ $Wm^{-2}$ | Ambient Temperature/℃ |
|---|---|---|---|---|---|
| *Test 1* | Hefei (31.83N, 117.25E) | 12:22/ 17.Dec.2017 | 1.2 | 714.3 | 7.5 |
| *Test 2* | | 15:14/ 17.Dec.2017 | 1.3 | 593.4 | 7.3 |

**Nomenclature**

| | | | |
|---|---|---|---|
| $C$ | Geometric concentration ratio | $T$ (K) | PV cell working temperature |
| $E_g$ (eV) | Material band-gap energy (1.124 eV for silicon) | $t_e$ (m) | the depth of the emitter |
| $FF$ (%) | Fill factor | $V$ (V) | Solar cell/module voltage |
| $G$ (W/m$^2$) | Illumination profile | $V_j$ (V) | Junction voltage |
| $I_{sc}$ (A) | Short-circuit current | $V_{oc}$ (V) | Open-circuit voltage |
| $J^e$ (A/m$^2$) | Current density | | |
| $K_b$ (J/K) | Boltzmann constant | **Greek symbols** | |
| $n$ | Diode ideal factor | $\Lambda$ (°) | A certain degree |
| $P_{max}$ (mW) | Maximum power | $\theta'$ (°) | The incidence angle for the optimization concentrator |
| $Q_j$ (A/m$^3$) | Generated current density | $\theta$ (°) | The incidence angle for the original concentrator |
| $q_e$ (C) | Electron charge | $\sigma$ (S/m) | Conductivity of the material |
| $R_{sh}$ ($\Omega$) | Sheet resistance | $\lambda$ (°) | Rotation angle |